

Received July 12, 2019; reviewed; accepted October 17, 2019

First-principles calculations of electronic structure of rhodochrosite with impurity

Guichun He ¹, Kun Li ¹, Tengbo Guo ¹, Shaoping Li ¹, Chaojun Huang ¹, Qinghua Zeng ²

¹ School of Resources and Environmental Engineering, Jiangxi University of Science and Technology, Ganzhou, Jiangxi 341000

² School of Computing, Engineering and Mathematics, Western Sydney University, Locked Bag 1797, Penrith, NSW 2751, Australia

Corresponding author: heguichun2006@163.com (Guichun He)

Abstract: The electronic structure of rhodochrosite containing impurity defects is studied by using the first principles density functional theory. The energy band structure, density of states and electronic distribution are calculated for rhodochrosite crystal models with various impurities (e.g., Cu, Ca, Mg, Zn, Fe). This paper discusses the effects of such defects on the electronic structure of rhodochrosite. The calculation results show that the impurity defects have a great impact on the surface electrical properties of rhodochrosite. For example, Ca and Mg impurities reduce the semiconductor width of rhodochrosite. Both Ca and Mg atoms in orbital bonding act as electron donors in which Ca3p and Mg2p orbits provide electrons while O2p orbits receive electrons. Moreover, the more number of valence electrons of Mn is the weaker covalent interaction between Mn and O atoms will be. Meanwhile, decrease of the total energy of rhodochrosite, makes the structure more stable. When Fe, Zn and Cu impurities are contained, the forbidden gap becomes narrower, which improves the conductivity of rhodochrosite. In addition, impurity bands will be formed in the 3d orbits of rhodochrosite as shown in its density of states, and the number of electrons in 3d orbits will increase. This weakens the covalence of O atoms, decreases the population values of O-Mn, increases the bond length, and enhances the ionicity of O-Mn bonds. The impurity of all defects considered in this study have shown an improved conductivity of rhodochrosite, and increased hole concentration of Mn atoms, which will be of great benefit to the adsorption of anionic collectors and enhance the electrochemical properties for rhodochrosite flotation process.

Keywords: rhodochrosite, first principles calculation, electronic structure, density of states

1. Introduction

Rhodochrosite is a manganese carbonate mineral that has a trigonal crystal structure. Yet, rhodochrosite in nature has a variable chemical composition and the manganese is frequently replaced by calcium, magnesium, iron, copper and zinc. Such substitution of impurity elements for manganese affects significantly the performance rhodochrosite flotation, which is a process of mineral concentration based on the difference of their surface chemical characteristics (Mao and Yong, 1994; Hong, 2011; Luo et al., 2018). Due to the diversity of conditions and environments during the mineral formation, rhodochrosite of different origins always has impurity defects to some degree.

The presence of impurities in the mineral crystal lattice affects the conductivity of minerals and thus affects the adsorption of flotation agents on mineral surface. The surface conductivity of minerals influences adsorption of agents on the mineral surface. When there are impurity atoms in the mineral lattice, these impurity atoms produce impurity bands, which provide space for electron transition. The impurity atoms affect the surrounding atoms by taking electrons from the surrounding atoms or giving them electrons, so as to affect the conductivity of the mineral or the mineral surface. Different types of impurities have different effects. Impurities are mainly divided into donor impurity and acceptor

impurity. Donor impurity is able to provide electrons, while acceptor impurity can gain electrons (Sholl and Steckel, 2009). It is necessary to study the effects of such impurity defects on the electronic conductivity of rhodochrosite and its flotation behaviors. It was reported that lattice defect affects significantly the floatation behaviors of metal sulfide ores (Chen, 2012). In addition, computational studies on pyrite, marcasite, sphalerite and galena demonstrated that lattice defect leads to the change of energy band structure, density of electronic states and atomic charge of these minerals (Xiao et al., 2001; Martin and Becker, 2006; He et al., 2006; Lei et al., 2007; Chen et al., 2010; Wu et al., 2015). Therefore, the study on crystal structure of minerals with impurity defects will help us to explain various flotation phenomena, to understand their flotation mechanisms, and to provide theoretical guidance for flotation practices.

With the development of computer technology, modelling and simulation have been applied to the studies of crystal structures and various parameters of minerals. For examples, the first-principles calculation was used to simulate the flotation separation of magnesite and quartz (Wu et al., 2015). Calculation and analysis were also conducted on triphylite with vacancies and impurity defects (Xu et al., 2016). Computer simulation has become an important tool to study crystal structures of materials. Some common simulation methods include the simulation of quantum mechanics (QM) (Johnson, 1975) and molecular dynamics (MD) simulation (Car, 1985). QM methods are mainly based on one-electron calculation, such as Hartree-Fock method (Fischer, 1977) and density functional theory (DFT) (Parr, 1990). DFT is the most common method since it replaces the basic variable of wave function with electronic density, which simplifies the calculation.

In this paper, DFT is applied to investigate the crystal structure of rhodochrosite with the impurity atoms of copper, calcium, magnesium, zinc and iron. GGA-RPBE exchange correction potential is adopted to calculate the influence of the energy band structures, the density of states, and the potential distribution on rhodochrosite doped the above impurity atoms. The effect of different impurity atoms on the interaction between rhodochrosite and reagent is also calculated by using the frontier orbit theory. This study is of great significance in enriching the flotation mechanism and guiding the flotation practice of rhodochrosite flotation.

2. Theoretical models and methodology

2.1. Theoretical models

The crystal models in present study are created from the crystal structure of rhodochrosite, whose space group has a R-3C trigonal system. A unit cell has 6 Mn, 6 C and 18 O atoms. The eight corners of a unit cell are occupied by manganese atoms and each corner is shared by three oxygen atoms. When considering the impurity defects, several models (Fig. 1) are created, with the formulas of $C_6O_{18}Mn_5Cu$, $C_6O_{18}Mn_5Ca$, $C_6O_{18}Mn_5Mg$, $C_6O_{18}Mn_5Zn$, and $C_6O_{18}Mn_5Fe$, respectively.

2.2. Calculation method

DFT calculation is performed by CASTEP module of Materials Studio 2017 (Segall et al., 2002). The Brodyden-Fletcher-Goldfarb-Shanno (BFGS) optimization algorithm is adopted for geometry optimization and property calculation. DFT exchange correlation function processing methods including LDA CA- PZ, GGA-WC, GGA-PW91, GGA-RPBE, GGA-PBE have different effect on the result of calculation (Table 1). The calculation shows that there are the minimum energy and the minor deviation of lattice parameters calculated by the function GGA-RPBE.

The Perdew-Burke-Ernzerhof generalized gradient approximation (GGA-RPBE) is used to describe the electronic exchange correlation function (Perdew et al., 1996). The plane wave cut-off energy for the ultra-soft pseudo-potential is set to 300eV. The Brillouin zone is sampled by using the Monkhorst-Pack scheme with grid of size $5 \times 5 \times 2$ K points. The energy convergence criterion of self-consistent operation is set to 2×10^{-6} eV/atom. Electronic valence states involved in the calculation are respectively $Mn3d^54s^2$, $O2s^22p^4$, $Cu3d^{10}4s^1$, $Ca3s^23p^6$, $Mg2p^63s^2$, $Zn3d^{10}4s^2$ and $Fe3d^64s^2$.

2.3. Result analysis

Several parameters are calculated by using the CASTEP properties task, including band structure, density of states (DOS), Mulliken population analysis, and partial density of states (PDOS). The bond structure describes the range of energies among which there may be (i.e., energy bands) or may not be (i.e., band gaps) an electron within a solid material. DOS describes the number of states per interval of energy at each energy level available to be occupied. Mulliken charges are calculated from Mulliken population analysis, which provides a way to estimate the partial atomic charge.

Table 1. The results of calculation by different functions

Function	Energy cut-off /eV	Lattice parameter / 10^{-9} m (deviations/ %)	Energy/ eV
GGA-PBE	300	a = b = 4.643 (2.6%) c = 15.168 (3.16%)	-12698.189
GGA-RPBE	300	a = b = 4.679 (1.92%) c = 15.069 (3.79%)	-12718.761
GGA-PW91	300	a = b = 4.639 (2.89%) c = 15.090 (3.66%)	-12717.121
GGA-WC	300	a = b = 4.593 (3.85%) c = 14.192 (9.39%)	-12672.547
LDA CA-PZ	300	a = b = 4.542 (4.9%) c = 13.860 (11.51%)	-12668.056

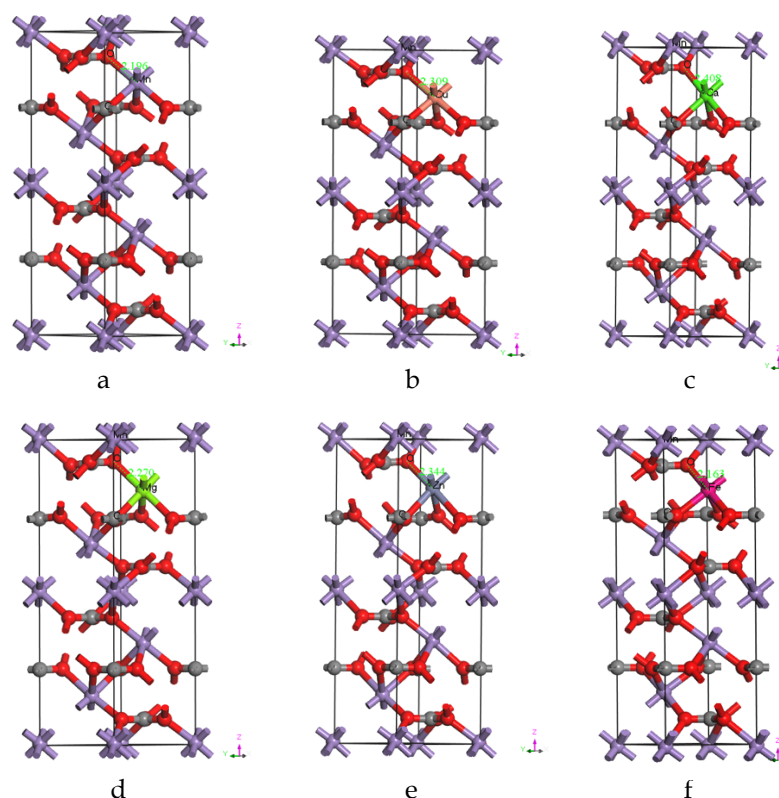


Fig. 1. Crystal models of rhodochrosite and those with impurity defects ($1 \times 1 \times 1$): (a) rhodochrosite, (b) Cu-rhodochrosite, (c) Ca-rhodochrosite, (d) Mg-rhodochrosite, (e) Zn-rhodochrosite, (f) Fe-rhodochrosite

3. Results and discussion

3.1. Energy band structure and density of states of rhodochrosite

Firstly, BFGS optimization algorithm is adopted to optimize the geometry of each rhodochrosite unit cell. Then, the energy band structure and density of states of rhodochrosite are obtained by DFT calculation. The density of states (Fig. 2) shows that rhodochrosite is a p-type semiconductor. Moreover, the highest energy point is not symmetric with the lowest energy point, which indicates that it is an indirect p-type semiconductor. The forbidden band width of 1.305eV suggests a certain electrical activity. The main component is O2s orbit at the low energy levels from -25eV to -24eV and from -22eV to -21eV. The main component is O2p orbits at the energy levels from -10eV to -7eV and from -6eV to -2eV. Such O2p orbits have a low density of states and their peak values are relatively close. Mn and O atomic orbits are the main contributors of Fermi level.

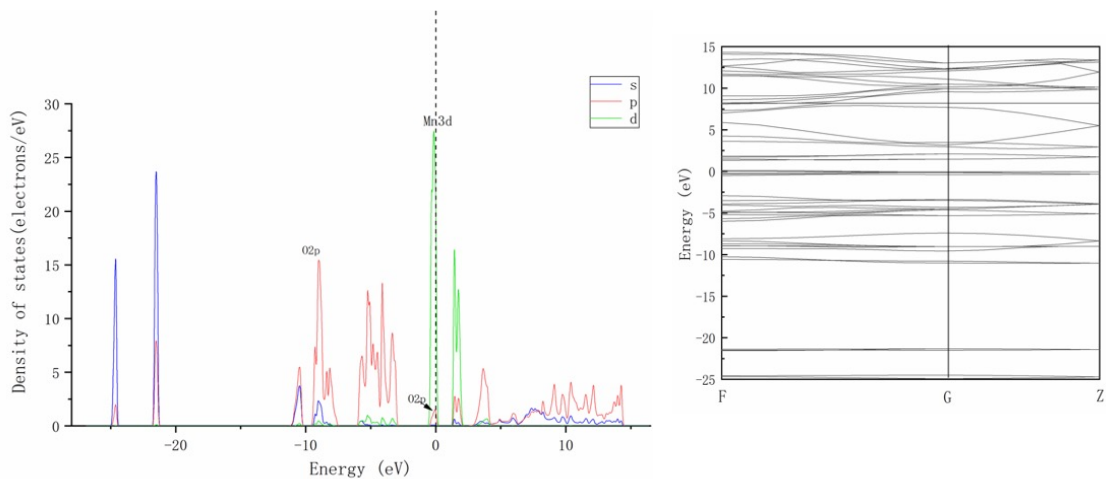


Fig. 2. Band structure and density of states of rhodochrosite

According to single-orbit density of states (Fig. 3), Fermi level is mainly contributed by Mn3d orbits. Therefore, the main electrochemical property of rhodochrosite is determined by Mn atoms. According to Mulliken population analysis that electrons mainly come from C2p orbits and Mn3d orbits during the formation of rhodochrosite crystals, the population analysis demonstrates a high electronic density of C-O bond, which indicates a nature of covalent bond. And a low electronic density of states of Mn-O bonds indicates an ionic bond property. The atomic charge numbers of Mn and O atoms are respectively 1.03e and -0.59e.

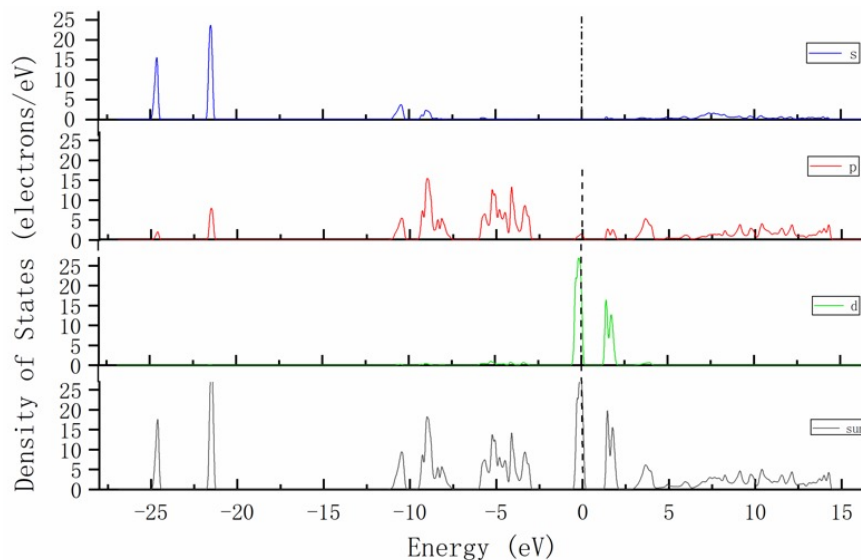


Fig. 3. Partial density of states of rhodochrosite

3.2. Energy band structure of rhodochrosite with impurity defects

Although rhodochrosite with Ca, Mg, Fe, Cu and Zn impurity does not show any obvious change of its conduction property, its forbidden bandwidth decreases, which promotes the conduction of electrons. Compared with the rhodochrosite without impurity, both of them have a certain decrease in forbidden band width, Therefore, the inclusion of such impurity defects activates rhodochrosite and improves its conductivity.

Mg and Cu have the weakest effect on the band gap of rhodochrosite, while Fe has the strongest. A relative smooth impurity band has been generated by all other impurity defects except for Mg impurity, which has a little influence on the crystal characteristics. Besides, these impurities decrease the overall system energy and increase the bond ionicity, which is consistent with the subsequent analysis of the population bond distribution.

Table 2. Band gap of rhodochrosite with various impurity defects

Impurity type	Cu	Ca	Mg	Zn	Fe
Band gap (eV)	1.20	1.12	1.20	1.17	0.60

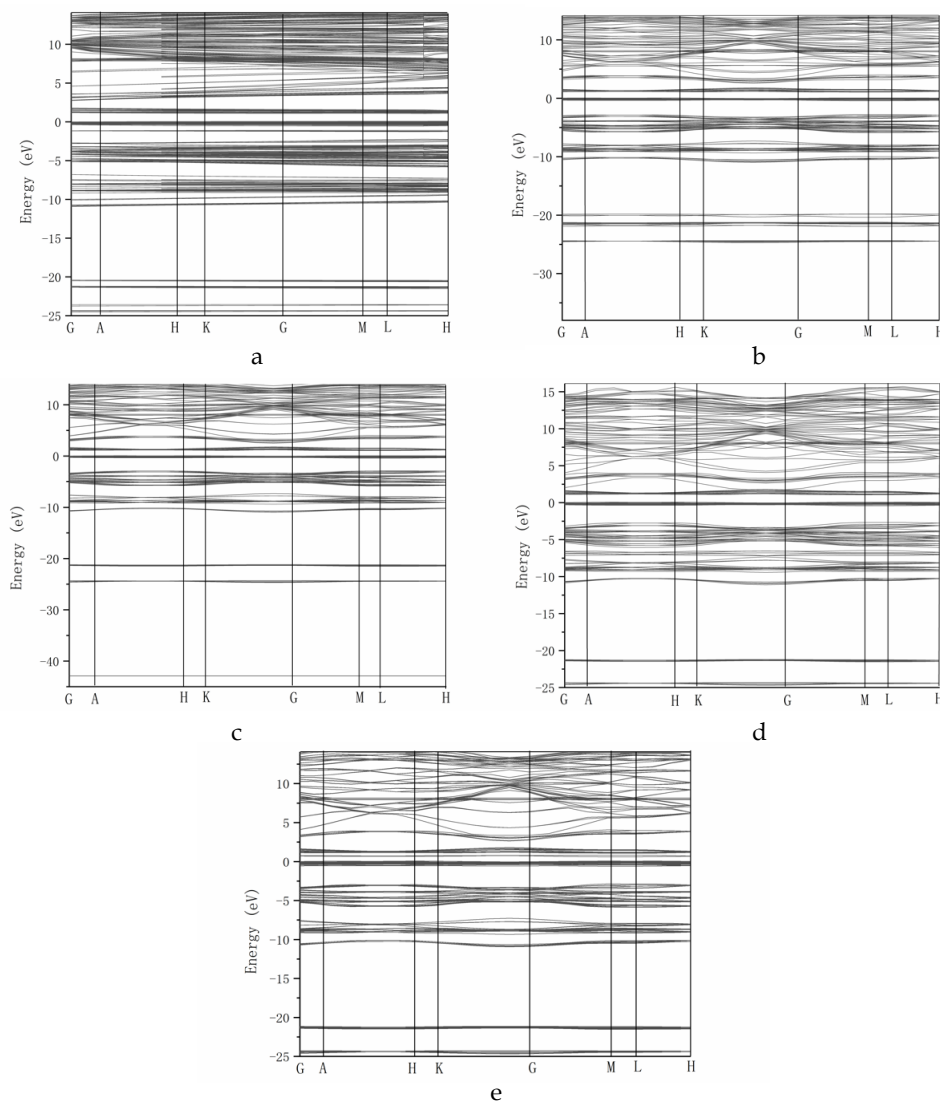


Fig. 4. Band structures of (a) Cu-rhodochrosite, (b) Ca-rhodochrosite, (c) Mg-rhodochrosite, (d) Zn-rhodochrosite, (e) Fe-rhodochrosite

3.3. Density of states of rhodochrosite with impurity defects

There is no obvious change of the density of states in rhodochrosite with impurity defects (i.e., Cu, Ca, Mg, Zn and Fe) (Fig. 5). Mn atoms remain the main contributor of Fermi level, without any obvious band offset. However, such defects cause impurity bands under a certain density of states. For example, defects of Cu, Fe and Zn impurities cause impurity band at low energy levels of -7eV to -2eV, -12eV to -6eV and -7eV to -2eV, respectively. A defect of Ca impurity causes a relatively smooth and negligible impurity band under the energy level of 3eV to 6eV. A defect of Mg impurity makes no contribution to the density of states in rhodochrosite and thus it is not involved in the exchange of electrons during reaction and does not contribute at all to Fermi level. Therefore, even under the presence of impurities the electrochemical properties of rhodochrosite are still dominated by Mn atoms. But, all impurities above have increased the number of surface electrons of Mn atoms, which will have an influence on the adsorption behaviors of anionic collectors on rhodochrosite.

The Mulliken population analysis has been performed for the atoms and bonds of pure rhodochrosite and that with various metallic impurities. Such analysis indicates the distribution of electrons in each atomic orbit, including overall population of the same orbit and the overlap population between two orbits. The electronic distribution within the energy band has a great influence on the chemical properties of minerals, which can also demonstrate the electronic transfer in bonding, the nature of ionic and covalent bonds. In general, bonds with a high population value and a short bond length are covalent, while those with a low population value and a long bond length are ionic.

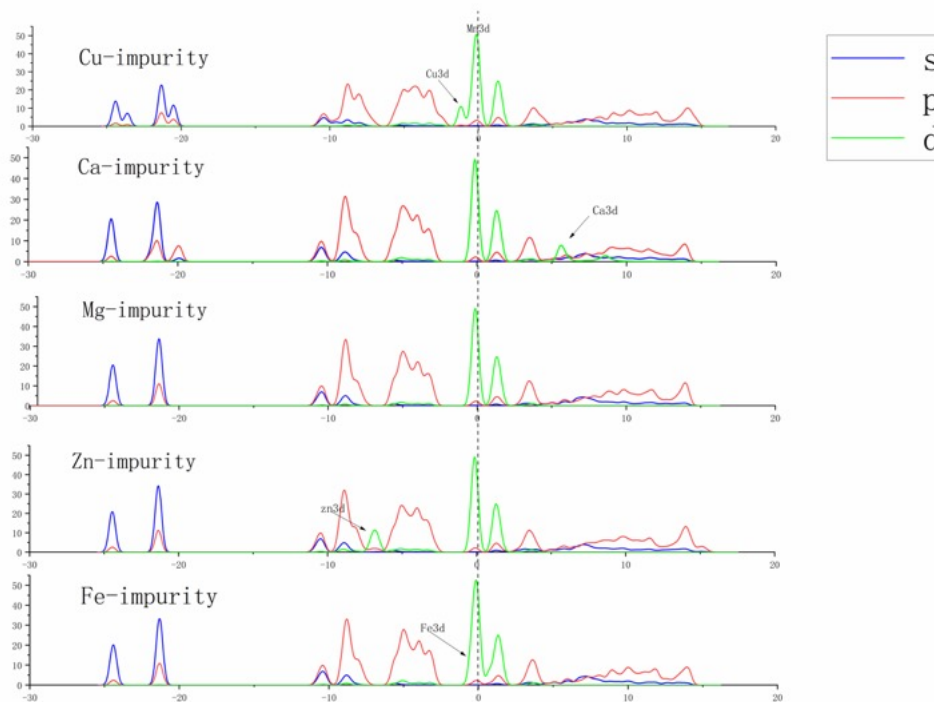


Fig. 5. Total density of states of rhodochrosite with various impurity defects

3.4. Mulliken population analysis of rhodochrosite with impurity defects

The Mulliken population analysis has been carried out for the atoms and bonds. In rhodochrosite, O atoms obtain electrons by treating O2p orbitals as an electron acceptor, while Mn and C atoms give electrons by treating Mn3d and C2p orbitals respectively as electron donors (Table 3). In rhodochrosite with metallic impurities (e.g., Cu, Ca, Mg, Zn and Fe), the number of electrons in Mn3d orbitals and C2p orbitals increases, which has great benefit to the conductivity and weakens their covalence between Mn and O atoms. At the same time, the defect metals act as electron donors, their d orbitals (e.g., Cu, Zn and Fe) or p orbitals (e.g., Mg, Ca) provide electrons to p orbitals of O atoms. It results in an obvious increase of the number of Mn3d orbital electrons and a decrease of that of valence electrons of Mn atoms. Thus, the covalence between Mn and O atoms is weakened.

Table 4 shows that bond population values of defect metals with O atoms are higher than that of Mn with O atoms, which may contribute to the increase of length of O-O and O-Mn bond, O-Mn ionicity, ionic activity of Mn atoms and instability of mineral crystals. Meanwhile, the defect metal tends to bind with O and form a metal-O bond. Table 4 also indicate that the bond population values and corresponding bond length of defect metal-O bonds are less than those of O-Mn bonds, but their own bond lengths are nearly the same, so they have the same ionic properties. Thus, the ionicity of defect metal-O bonds is higher than that of O-Mn bonds. The above results manifest that metallic defect in rhodochrosite will weaken the covalence between Mn and O atoms, and enhance the mineral conductivity.

Table 3. Atomic population distribution of rhodochrosite with various impurity defects

Type of defects	Atom	s orbit	p orbit	d orbit	Total	Charge (e)
rhodochrosite	C	0.84	2.24	0	3.26	0.74
	O	1.79	4.8	0	6.59	-0.59
	Mn	0.26	0.15	5.56	5.97	1.03
Cu-rhodochrosite	C	0.85	2.41	0	3.26	0.74
	O	1.8	4.79	0	6.59	-0.59
	Mn	0.41	0.16	5.71	6.28	0.72
	Cu	1.04	0.03	9.46	10.52	0.48
Ca-rhodochrosite	C	0.85	2.41	0	3.22	0.74
	O	1.79	4.8	0	6.59	-0.59
	Mn	0.36	0.24	5.82	6.43	0.57
	Ca	1.55	5.64	2.09	9.28	0.72
Mg-rhodochrosite	C	0.84	2.41	0	3.22	0.74
	O	1.79	4.79	0	6.59	-0.73
	Mn	0.42	0.25	5.82	6.49	0.51
	Mg	2.34	6.24	0	8.58	1.42
Zn-rhodochrosite	C	0.85	2.41	0	3.27	0.78
	O	1.79	4.79	0	6.59	-0.59
	Mn	0.43	0.17	5.66	6.27	0.73
	Fe	0.92	-0.14	6.96	7.74	0.26

Table 4 Bond population distribution of the defective rhodochrosite

Type of defects	Atom	Bond	Population value	Length (Å)
rhodochrosite	C	C-O	0.89	1.2769
	O	O-O	0.21	2.21166
	Mn	O-Mn	0.2	2.17086
Cu-rhodochrosite	C	C-O	0.88	1.286
	O	O-O	0.2	2.2658
	Mn	O-Mn	0.21	2.19573
	Cu	O-Cu	0.57	2.22741
Ca-rhodochrosite	C	C-O	0.77	1.286
	O	O-O	0.2	2.22741
	Mn	O-Mn	0.21	2.19573
	Ca	O-Ca	0.39	2.22741
Mg-rhodochrosite	C	C-O	0.89	1.286
	O	O-O	0.2	2.2658
	Mn	O-Mn	0.21	2.19573
	Mg	O-Mg	0.44	2.22741
Zn-rhodochrosite	C	C-O	0.82	1.30816

	O	O-O	0.2	2.2658
	Mn	O-Mn	0.21	2.19573
	Zn	O-Zn	0.54	2.22741

3.5. Frontier molecular orbital analysis of rhodochrosite with impurity defects

Based on the frontier orbital theory (Houk, 1975), electrons are usually given from the highest orbital of the collector molecule and the lowest orbital of the mineral during flotation. The absolute value of difference in orbital energy ($|\Delta E|$) is calculated from subtracting reagent from mineral. The smaller the difference $|\Delta E|$ is, the stronger the reaction between the reagent with the mineral is. The frontier orbital energy of rhodochrosite and sodium oleate is shown in table 5. It can be seen from table 5 that the difference of energy of rhodochrosite with impurities and sodium oleate decreases to different degrees compared with that of rhodochrosite without impurities, which proves that the rhodochrosite with impurity defects is conducive to the adsorption of anionic collectors.

Table 5. Influence of impurity on front orbital energy of rhodochrosite

	$E_{\text{HOMO}}/\text{eV}$	$E_{\text{LUMO}}/\text{eV}$	$ \Delta E_1 /\text{eV}$
Rhodochrosite	-4.375	-3.540	1.344
Ca-rhodochrosite	-4.572	-3.742	1.142
Mg-rhodochrosite	-4.716	-3.856	1.028
Zn-rhodochrosite	-4.732	-4.209	0.675
Fe-rhodochrosite	-4.454	-3.763	1.121
Cu-rhodochrosite	-4.729	-3.867	1.017
Sodium oleate	-4.884	-1.324	

$$|\Delta E_1| = |E_{(\text{HOMO Sodium oleate})} - E_{(\text{LUMO Rhodochrosite})}|$$

4. Conclusions

The First principle calculation has been performed to study the electronic structure of rhodochrosite and those with impurity defects. The results show that impurity defects will change the energy band structure, electronic density of states and charge distribution of rhodochrosite, specifically, which will finally affect its chemical properties and flotation behaviors.

- Impurity defects have a great influence on the surface conductivity of rhodochrosite such as changing the semiconductor properties of rhodochrosite, which is beneficial to the adsorption of reagents on rhodochrosite. Such defects also have a certain influence on the bonding of rhodochrosite crystal by reducing its total energy and making the crystal structure stable.
- For rhodochrosite with Ca or Mg impurities, it's impurity contribution of rhodochrosite is that p channel of Ca and Mg provides electrons while d channel does not play its role, which changes the energy band structure of rhodochrosite and also improves the conductivity of electrons. Then, the covalence of Mn and O atoms will be weakened. The Mn-O bond length will increase and the number of valence electrons of Mn atoms will decrease.
- Rhodochrosite with Fe, Zn and Cu atoms will lead to a decrease in energy gap and the formation of impurity bands around Fermi level that connects conduction bands and valence bands. Such impurity band will reduce the electron number of Mn3d orbits, weaken their covalent with oxygen, and increase the population value of O-Mn bonds. The impurity bond length formed by impurity and oxygen is the same as that formed by oxygen and manganese atoms, and then it will affect the flotation of rhodochrosite finally.
- The above impurity defects in rhodochrosite will decrease the number of valence electrons of Mn and increase the number of positive charges, which will have a benefit to the adsorption of anionic collectors on mineral surface. This conclusion is eventually confirmed by the calculation of the frontier orbital energy.

Acknowledgements

The authors gratefully acknowledge the financial support of National Natural Science Foundation of China (No.51774152) as well as Science and Technology Innovation Talents of Jiangxi Province (No. S2017RCCXB0002).

References

- HONG, S. 2011. *Status of China Mn-ore in Resources Exploitation and the Sustainable Development*. China's manganese industry, 29(3), 13-16.
- MAO, J., ZHANG, Y., 1994. *Effects of multivalent metal Ions on floatability of rhodochrosite*. China's manganese industry, 12(6), 23-28.
- LOU, N., WEI, D.Z., SHEN, Y.B., LIU, W., GAO, S.L., 2011 *Effect of calcium ion on the separation of rhodochrosite and calcite*. Journal of Materials Research and Technology, 7(1), 96-101.
- SHOLL, D.L., STECKEL, J.A., 2009. *Density Functional Theory a Practical Introduction*. John Wiley & Sons, Inc., p. 243
- CHEN, J.H., 2012. *Principles of the flotation of sulphide minerals bearing lattice defects*. Central South University Press, 321
- CHEN, J.H., ZENG, X.Q., CHEN, Y., ZHANG, H.P., 2010. *First-principle theory calculations of electronic structure of sphalerite with vacancy and impurity*. The Chinese Journal of Nonferrous Metals, 20(4), 765-771.
- MARTIN, R., BECKER, U., 2006. *First-principles calculations of the thermodynamic mixing properties of arsenic incorporation in to pyrite and marcasite*. Chem. Geol., 225(3/4), 278-290.
- HE, K.H., YU, F., JI, G.F., YAN, Q.L., ZHENG, S.K., 2006. *Study of Optical Properties and Electronic Structure of V in ZnS by First Principles*. Chinese Journal of High Pressure Physics, 20(1), 56-59.
- XIAO, Q., QIU, G.Z., HU, Y.H., 2001. *Computational simulation to mechanical activation of pyrite (I) - Relation of structural strain to chemistry reaction activity*. The Chinese Journal of Nonferrous Metals, 11(5), 900-904.
- LEI, Y. HU, X.Q., LIU, J.D., 2007. *Influence of the structural electronic and optical properties on ZnS doped Co*. Journal of Nanchang University, 31(6), 564-565.
- WU, G.Y., ZHU, Y.G., YAN, Z.G., ZHENG, G.B., TAN, X., LIU, G.C., ZHANG, J., 2015. *First Principles Study on flotation separation of magnesite and quartz*. Mining & Metallurgy, 24(2), 11-14.
- OERTZEN, G., JONES, R.T., GERSON, A.R., 2005. *Electronic and optical properties of Fe, Zn and Pb sulfides*. Physics and Chemistry of Minerals, 32, 255-268.
- XU, C., LI, W., HE, X., SHANG, Y., 2016. *First-Principles Calculations of Electronic Structure of LiFePO₄ with Vacancy and Impurity*. Chemistry Bulletin, 79(5), 412-417.
- JOHNSON K.H., 1975. *Effect of calcium ion on the separation of rhodochrosite and calcite*. Quantum Chemistry. Annual Review of Physical Chemistry, 26(26), 39-57.
- CAR, R. 1985. *Unified Approach for Molecular Dynamics and Density-Functional Theory*. Phys. Rev. Lett., 55(22), 24-71.
- FISCHER, C.F., 1977. *The Hartree-Fock method for atoms*. Wiley, pp. 308.
- PARR, R.G., 1990. *Density Functional Theory*. Chemical & Engineering News, 68(1), 45.
- SEGALL, M.D., LINDAN, P.J.D., PROBERT, M.J., PICKARD, C.J., HASNIP, P.J., CLARK, S.J., PAYNE, M.C., 2002. *First-principles simulation: Ideas illustrations and the CASTEP code*. J. Phys. Cond. Matter, 14, 2717-2743.
- PERDEW, J.P., BURKE, K., ERNEZERHOF, M. 1996. *Generalized gradient approximation made simple*. Phys. Rev. Lett., 77, 3865-3868.
- HOUK, K.N., 1975. *Frontier molecular orbital theory of cycloaddition reactions*. Accounts of Chemical Research, 8(11), 361-369.